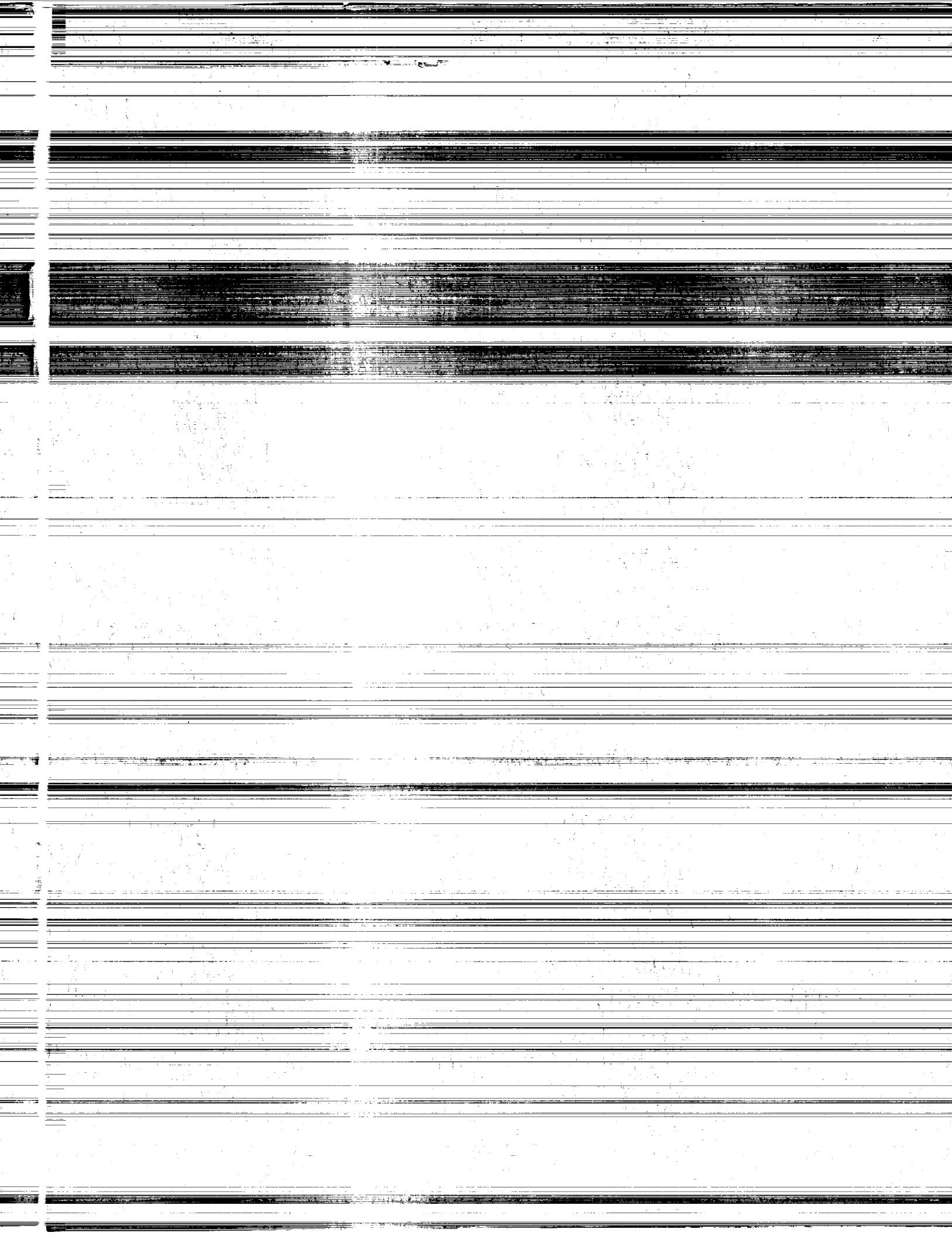p. 15

Modeling of the Heat Transfer in Bypass Transitional Boundary-Layer Flows

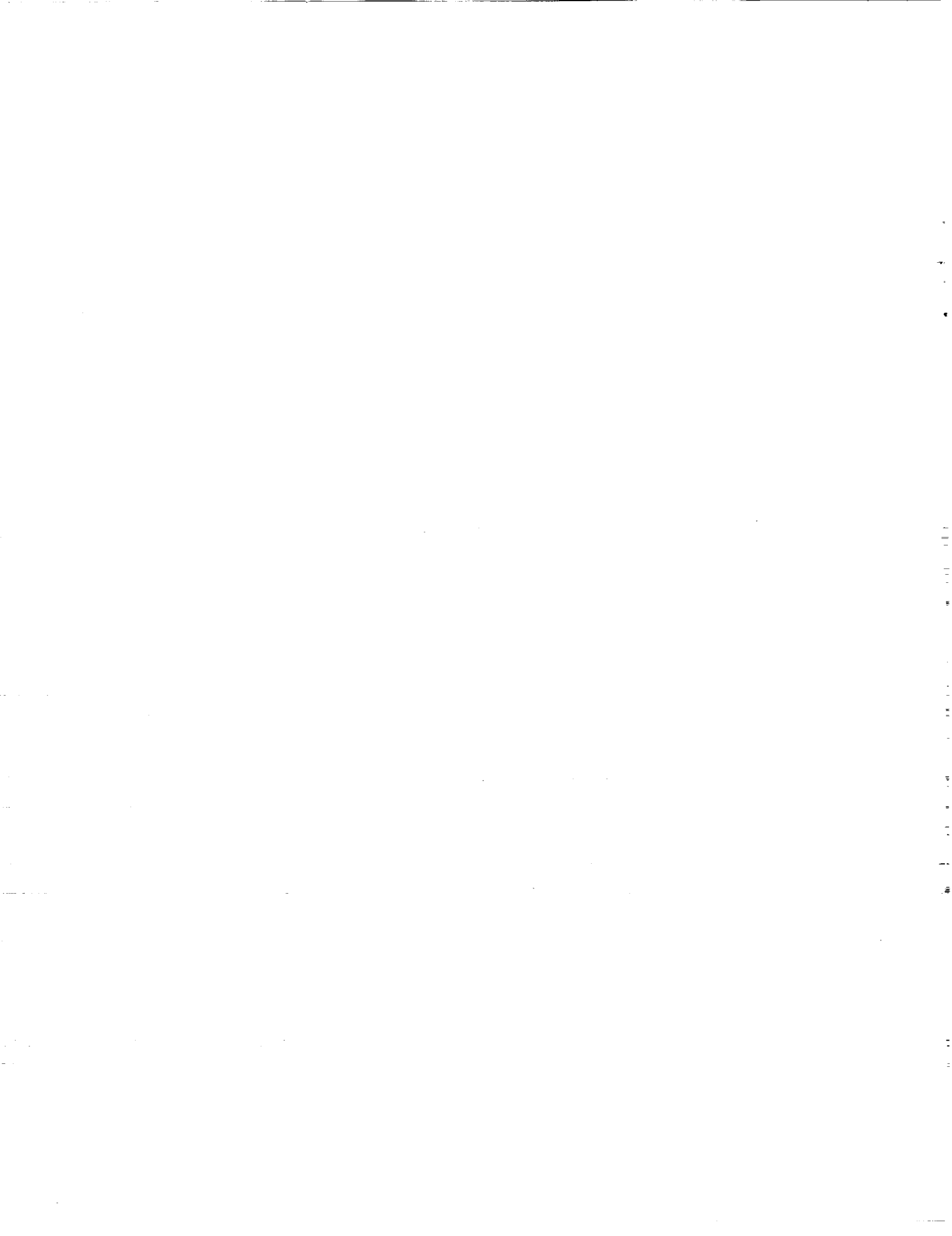Frederick F. Simon
and Craig A. Stephens

NASA

Modeling of the Heat Transfer in Bypass Transitional Boundary-Layer Flows

Frederick F. Simon
Lewis Research Center
Cleveland, Ohio

Craig A. Stephens
PRC, Inc.
Edwards, California

Summary

A low Reynolds number k-ϵ turbulence model and conditioned momentum, energy and turbulence equations were used to predict bypass transition heat transfer on a flat plate in a high-disturbance environment with zero pressure gradient. The use of conditioned equations has been demonstrated by other researchers to be an improvement over the use of the global-time-averaged equations for the calculation of velocity profiles and turbulence intensity profiles in the transition region of a boundary layer. The present work extends the approach of conditioned equations to include heat transfer and uses a modeling of transition events to predict transition onset and the extent of transition on a flat plate. These events, which describe the boundary layer at the leading edge, result in boundary-layer regions consisting of (1) the laminar, (2) pseudolaminar, (3) transitional, and (4) turbulent boundary layers. The modeled transition events were incorporated into the TEXSTAN two-dimensional boundary-layer code which is used to numerically predict the heat transfer. The numerical predictions in general compared well with the experimental data and revealed areas where additional experimental information is needed.

Introduction

The transition from laminar to turbulent boundary-layer flow effects great increases in the local wall shear stress and heat transfer. This effect of transition is especially critical for airfoil surfaces such as turbine blades where 50 percent or more of the blade surface can be in transition. The ability to predict the starting location and streamwise extent of transition is important to the determination of turbine blade heat transfer that critically affects longevity and engine performance. The accurate prediction of gas-side heat transfer on turbine blades will become more critical as the desired operating temperatures and stage loading levels of advanced turbine engines increase. The present methods for predicting transition shear stress and heat transfer on turbine blades are based on incomplete knowledge. Little is known about the transition process in an engine environment where disturbance levels are initially large. In such a large disturbance environment, traditional linear mechanisms are bypassed and finite, nonlinear effects must be considered.

Modeling of this transition phenomena to predict wall shear stress and heat transfer on turbine blades must consider the effects of free-stream turbulence, pressure gradient, streamwise curvature, surface roughness, wall and free-stream temperature ratio and flow disturbances (e.g., wakes). In the present work the effect of free-stream turbulence on the computation of transition heat transfer on a flat plate is investigated.

Computational models for the calculation of wall shear stress and heat transfer in transition flows may be classified into four groups (Narasimha, 1985). These groups are linear combination models, algebraic models, differential models, and higher order models. Linear combination models calculate overall shear stress and heat transfer in terms of a linear combination of the intermittent laminar and turbulent properties of the transition boundary layer. Examples of this group are Dhawan and Narasimha (1958), Chen and Thyson (1971), and Dey and Narasimha (1988). Algebraic models use an algebraic model for the Reynolds stress of the time-averaged equations of motion. By gradually turning on the turbulent viscosity in proportion to the intermittency, it becomes possible to simulate the transition from a laminar to turbulent boundary layer. Such a model requires knowledge of the start of transition, the transition length, and the transition path. Examples of this are Cebeci and Smith (1974) and Gaugler (1985). Differential models describe the Reynolds stress of the time-averaged equations by the use of one- or two-equation turbulence closure models. The one-equation model determines a turbulent velocity scale with a turbulent kinetic energy equation with the length scale determined algebraically. The two-equation model determines the length scale with an additional partial differential equation. The most well-known two-equation model is the Jones and Launder (1973) k-ϵ model. Examples of this model for simulating transition in a high-disturbance environment are given by Rodi and Scheurer (1985) and Schmidt and Patankar (1988). Higher order models do not use the eddy viscosity concept to calculate Reynolds stresses (as required in the above three models), but rather use differential equations for each of the Reynolds stresses. Donaldson (1969) performed a two-dimensional boundary-layer analysis with higher order equations to determine the effect of large disturbances on transition. Differential models require a knowledge of the starting location of the initial profiles to determine the correct location of the beginning of transition. The work of Schmidt and Patankar (1988) is an example of the importance of locating these initial profiles in transition calculations.

The present work uses a low Reynolds number, k-ϵ turbulence model for calculating the transition heat transfer in

environments of high disturbance. In general, k-ϵ two-equation models simulate the transition governed by the transport of turbulence from the free stream into the boundary layer. However, previous results of this approach for flat-plate heat transfer have underpredicted the transition length and inconsistently predicted the start and finish of transition (Rodi and Scheurer, 1985). To address these problems and to make predictions consistent with the experimental evidence, Schmidt and Patankar (1988) modified the turbulent production term in the differential equation for the turbulent kinetic energy (k) and assumed the presence of an initial laminar boundary layer.

The present approach divides transition into four regions for the purpose of applying a model to the physics of each region: (1) the laminar boundary layer (2) the pseudolaminar (3) the transition and (4) the turbulent boundary layers. The conditions for determining the existence of each region will be presented. Models will be given for determining disturbance growth in region 2 and describing the presence of turbulent spots in region 3. Numerical predictions are made using the TEXSTAN boundary-layer computer code (Crawford, 1985). TEXSTAN is based on the STAN5 boundary-layer program developed by Crawford and Kays (1976). The finite difference scheme of TEXSTAN is based on the numerical algorithm by Patankar and Spalding (1970). TEXSTAN solves the steady two-dimensional parabolic differential equations that govern boundary-layer flow. This program sequentially solves the momentum equation and any number of transport equations such as stagnation enthalpy, turbulent kinetic energy (TKE), turbulent dissipation rate (TDR), and mass concentration governing equations. Numerical predictions are compared with the flat-plate, zero pressure gradient data of Blair and Werle (1980).

Symbols

C_μ, C_1, C_2	constants appearing in the k-ϵ turbulence model
c_v, c_T, c_k	model constants for source terms
c_f	skin friction
f_2, f_μ	low Reynolds number functions
I	intermittency function
K	thermal conductivity
k	turbulence kinetic energy
L_e	dissipation length scale
L_{tr}	transition length
N	nondimensional spot formation rate
n	spot formation rate
Pr_t	turbulent Prandtl number
p	static pressure
q_w	wall heat flux
Re_θ	momentum thickness Reynolds number
St	Stanton number

T	temperature
T'	fluctuating temperature
Tu	turbulence intensity
$\overline{T'v'}$	turbulent heat flux
t	time
U_e	free-stream velocity
$u, v, w,$	mean velocity in x,y,z directions
u', v', w'	fluctuating velocities in x,y,z directions
$\overline{u'v'}$	turbulent shear stress
x_{tr}	location of transition onset (spot formation begins)
γ	intermittency
δ^*	displacement thickness
δ_3	energy thickness
ϵ	dissipation rate
θ	boundary-layer momentum thickness
Λ	longitudinal integral length scale
λ	thermal conductivity/specific heat
μ	molecular viscosity
μ_t	eddy or turbulent viscosity
ρ	fluid density
σ	dependence area factor
$\sigma_k, \sigma_\epsilon$	empirical constants in turbulence model

Subscripts:

e	denotes free-stream value
l	laminar zone of transition region
t	turbulent zone of transition region
tr	transition

Analysis

The boundary layer flow is assumed to be steady, incompressible, and two-dimensional. Spanwise variations are neglected.

Figure 1 depicts the development of a boundary layer in x-y coordinates. For purposes of modeling, the growth of the boundary layer is described in terms of regions. Region 1 is the laminar boundary layer, where small disturbances introduced into this layer are damped. Experimental evidence suggests that this region is nonexistent for free-stream turbulence levels greater than 5 percent. Region 2, which begins when the critical Reynolds number for linear instability is reached, represents the growth of nonlinear disturbances and extends from the critical Reynolds number to the position where the turbulent spots begin. In region 2, according to Morkovin

Region
1 Laminar boundary layer
2 Psuedo-Laminar
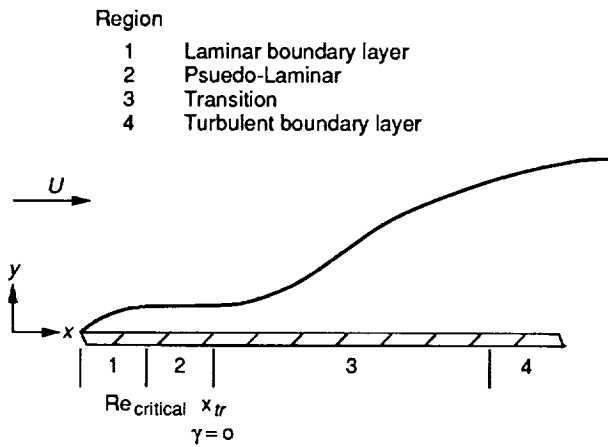3 Transition
4 Turbulent boundary layer

Figure 1.—Transition model.

(1978), when large disturbances exist, linear stability mechanisms are bypassed and finite, nonlinear instabilities occur. Because this region may have characteristics of a laminar boundary layer, it is called the pseudolaminar region. The growth of unstable waves in region 2 eventually results in the formation of turbulent spots (region 3). In region 3, the beginning and development of turbulent spots, there is an intermittent appearance of turbulent spots that grow as they move downstream until they finally merge to form the turbulent boundary layer (region 4). Each of these regions will be considered separately.

Region 1 (Laminar Boundary Layer)

The work of Abu-Ghannam and Shaw (1980) indicates that the transition momentum Reynolds number decreases to an asymptotic value of 163 for increases in the free-stream turbulence intensity. This Reynolds number value suggests that region 1 is governed by considerations of linear stability or Tollmien-Schlichting stability. Contrary evidence for high disturbance levels is indicated by some recent work (Rued and Wittig, 1985; Blair and Werle, 1980; Sohn, Reshotko, and O'Brien, 1989). These results indicate that the onset of transition begins close to the leading edge of a flat plate for free-stream turbulence intensity greater than about 5 percent. Rued and Wittig theorized that the lack of a minimum asymptotic transition Reynolds number for his results was due to the use of a thin leading edge. They speculated that the acceleration effects of thick leading edges provide additional stability. Such differences would be important when applying flat-plate transition information to turbine design.

Elder (1960) demonstrated that below the critical Reynolds number for stability, the flow was stable to small disturbances but unstable to large disturbances. He determined that breakdown to turbulent spots would occur for boundary-layer velocity fluctuations greater than 18 percent of the free-stream velocity. He found this event to be independent of the Reynolds number, and he postulated that the Reynolds number was important in the growth of the disturbances.

Dyban's experiments (1976) on a flat plate suggest that disturbances of the order determined by Elder for transition to occur are present near the leading edge for free-stream turbulence intensities of 4½ percent or more. The evidence, therefore, suggests that in cases where additional stabilization (e.g., acceleration) is not present, region 1 is essentially nonexistent for free-stream intensities of 5 percent or more. This is consistent with the statement of Reshotko (1986) that transition can occur at Reynolds numbers lower than the Reynolds for the onset of linear growth when initial disturbance is large enough to be nonlinear. According to Reshotko (1986) who cites the experimental data of Sohn (1986), the onset of nonlinear boundary-layer disturbance growth for 2 percent free-stream turbulence begins at a momentum Reynolds number of 96. This suggests that the onset of nonlinear growth is dependent on the level of the free-stream turbulence. However, the transition Reynolds number of 96 measured by Sohn is too low. Sohn attributes his value to possible adverse pressure gradient effects. Until definitive experimental evidence is provided, the present work assumes that nonlinear boundary-layer disturbance growth begins at the Reynolds number for the linear stability limit.

Critical momentum Reynolds numbers of 163 and 200 are generally used for the onset of instability, with 200 being considered the more accurate value. However, for the present study a value of 163 is used for consistency with the asymptotic limit at high turbulence intensities reported by Abu-Ghannam and Shaw (1980).

The following criteria are used for region 1:
1. No stabilizing effects present at the leading edge
   a. $Tu_e < 5$ percent; disturbance growth (region 2) begins at $Re_\theta = 163$
   b. $Tu_e > 5$ percent; disturbance growth begins at leading edge
2. Stabilizing effects present at leading edge; disturbance growth begins at $Re_\theta = 163$.

Region 2 (Pseudolaminar)

Region 2 requires that we analytically describe the amplification of boundary-layer disturbances in conjunction with the momentum and energy equations for the boundary layer. Dey and Narasimha (1984) proposed that transition is turbulence-driven for turbulence intensity levels greater than 0.1 percent. For levels less than this value, transition is said to be controlled by the availability of nonturbulent disturbances such as noise and vibration. This suggests that bypass transition and the amplification of disturbance energies (Reynolds stresses) can be described by turbulence models which determine the convection, diffusion and production of turbulence energy in the boundary layer. The equations to be used for region 2 are the boundary-layer equations for momentum and energy and the Jones-Launder (1973) two-equation turbulence model. These equations are given in the following sections:

3

Boundary-layer equation.—The flow is assumed to be steady and two-dimensional neglecting spanwise variations.

Momentum equation:

$$\rho u \frac{\partial u}{\partial x} + \rho v \frac{\partial u}{\partial y} = \frac{\partial}{\partial y}\left(\mu \frac{\partial u}{\partial y} - \rho \overline{u'v'} \right) - \frac{dp}{dx} \qquad (1)$$

where

$$-\rho \overline{u'v'} = \mu_t \frac{\partial u}{\partial y} = \left(\frac{C_\mu f_\mu \rho k^2}{\epsilon} \right) \frac{\partial u}{\partial y} \qquad (2)$$

Energy equation:

$$\rho u \frac{\partial T}{\partial x} + \rho v \frac{\partial T}{\partial y} = \frac{\partial}{\partial y}\left(\lambda \frac{\partial T}{\partial y} - \rho \overline{v'T'} \right) \qquad (3)$$

where

$$-\rho \overline{v'T'} = \frac{\mu_t}{\mathrm{Pr}_t} \frac{\partial T}{\partial y} \qquad (4)$$

Jones-Launder turbulence model.—Turbulence kinetic energy:

$$\rho u \frac{\partial k}{\partial x} + \rho v \frac{\partial k}{\partial y} = \frac{\partial}{\partial y}\left[\left(\mu + \frac{\mu_t}{\sigma_k} \right) \frac{\partial k}{\partial y} \right] - \mu_t \left(\frac{\partial u}{\partial y} \right)^2$$
$$- \rho \epsilon - 2\mu \left(\frac{\partial k^{1/2}}{\partial y} \right)^2 \qquad (5)$$

Turbulence dissipation:

$$\rho u \frac{\partial \epsilon}{\partial x} + \rho v \frac{\partial \epsilon}{\partial y} = \frac{\partial}{\partial y}\left[\left(\mu + \frac{\mu_t}{\sigma_\epsilon} \right) \frac{\partial \epsilon}{\partial y} \right] + C_1 \frac{\epsilon}{k} \mu_t \left(\frac{\partial u}{\partial y} \right)^2$$
$$- \frac{C_2 f_2 \rho \epsilon^2}{k} + 2.0 \frac{\mu \mu_t}{\rho} \left(\frac{\partial^2 u}{\partial y^2} \right)^2 \qquad (6)$$

Constants for the turbulence model are give in table I.

Region 3 (Transition)

Region 3, the transition region, is characterized by the intermittent appearance of turbulent spots which grow as they move downstream until they finally merge to form the turbulent boundary layer. The beginning of the transition region is defined by the first appearance of turbulence spots. Numerically this is assumed to occur when the calculations for region 2 show a rapid increase in turbulence kinetic energy k which results in an increase in the skin friction. Vancoillie and Dick (1988) state that conventional turbulence models

TABLE I.—CONSTANTS AND FUNCTIONS FOR JONES-LAUNDER TURBULENCE MODEL

(a) k-ϵ Turbulence model constants

C_μ	0.09
C_1	1.45
C_2	2.0
σ_k	1.0
σ_ϵ	1.3

(b) Functions

f_μ	$\exp\left[-2.5/(1 + R_T/50) \right]$
f_2	$1.0 - 0.3 \exp - R_T^2$
R_T	$\rho u l / \mu = \rho k^2 / \epsilon \mu$

based on global time averages can not give a good description of such intermittent flow, resulting in poor agreements for the turbulence intensity profiles for the boundary layer. They reported that using conditional averaging techniques for the turbulent spots and the laminar-like fluid surrounding the spots resulted in a good prediction of the experimental values of the velocity profiles and the turbulence intensity profiles in the transition region. As stated previously, turbulence models based on global averages underpredict the transition length. Schmidt and Patankar (1988) corrected this by using an empirical modification of the turbulence production term.

The present work extends the conditioned equation method of Vancoillie and Dick to include the energy equation for predicting heat transfer in the transition region. The conditioned momentum, energy, and turbulence equations for the turbulent spot and nonturbulent (laminar) portion of the intermittent flow in the transition region are combined and simplified to obtain global values of velocity and temperature. This permits use of the boundary-layer TEXSTAN code. Details of the analysis are presented in the appendix. The equations developed in the appendix (eqs. (A-12) and (A-23)) permit a consideration of the Reynolds stresses in the nonturbulent (laminar) zone. However, as assumed by Vancoillie and Dick and verified by the works of Sohn and Reshotko (1991) and Kim, Simon, and Kestoras (1989) for a flat plate with zero pressure gradient, the Reynolds stresses of the laminar zone can be neglected. As shown in the appendix, when the modeled equations for the turbulent and laminar zones are combined and the assumption made of negligible Reynolds stresses in the laminar zone, the following momentum and energy equations are obtained:

$$\rho u \frac{\partial u}{\partial x} + \rho v \frac{\partial u}{\partial y} = \frac{\partial}{\partial y}\left(\mu \frac{\partial u}{\partial y} - \gamma \rho \overline{(u_t' v_t')}_t \right) - \frac{dp}{dx}$$
$$+ \gamma \rho (u_l - u_t) \left[\frac{\partial u_t}{\partial x} - \frac{\partial u}{\partial x} \right] + \gamma \rho (v_l - v_t) \left[\frac{\partial u_t}{\partial y} - \frac{\partial u}{\partial y} \right] \qquad (7)$$

4

$$\rho u \frac{\partial T}{\partial x} + \rho v \frac{\partial T}{\partial y} = \frac{\partial}{\partial y}\left[\lambda \frac{\partial T}{\partial y} - \rho\gamma\overline{(v_l'T_l')}_l\right]$$

$$+ \rho\gamma(u_l - u_t)\left[\frac{\partial T_l}{\partial x} - \frac{\partial T}{\partial x}\right] + \rho\gamma(v_l - v_t)\left[\frac{\partial T_l}{\partial y} - \frac{\partial T}{\partial y}\right] \tag{8}$$

Equation (7) shows the Reynolds stresses multiplied by the intermittency factor. This is a form used by McDonald and Fish (1973) and others. A comparison of equations (7) and (1) indicates additional source terms as a result of spot formation. A comparison of equations (8) and (3) indicates the need to consider additional source terms because of the presence of a turbulent zone and a laminar zone in the transition region. These equations are simplified to permit the use the boundary-layer code TEXSTAN. The simplified equations also permit an evaluation of the additional source terms and of the validity of simplifying assumptions. The following assumptions are made for the momentum and energy equations:

$$\frac{\partial u_l}{\partial y} = \frac{\partial u}{\partial y}; \quad \frac{\partial u_l}{\partial x} = \frac{\partial u}{\partial x}$$

$$\frac{\partial T_l}{\partial y} = \frac{\partial T}{\partial y}; \quad \frac{\partial T_l}{\partial x} = \frac{\partial T}{\partial x} \tag{9}$$

The assumption for the velocity profile was also made by McDonald and Fish (1973) in their development of a turbulence model for transition. This assumption becomes more applicable as intermittency increases and velocity profiles become more turbulent. The errors introduced by this assumption should not be too large in the early part of transition because of the small value of intermittency. The result of these assumptions, as applied to equations (7) and (8), is the modification of equations (1) and (3) with the intermittency factor as follows:

$$\rho u \frac{\partial u}{\partial x} + \rho v \frac{\partial u}{\partial y} = \frac{\partial}{\partial y}\left(\mu \frac{\partial u}{\partial y} - \gamma\rho\overline{(u_l'v_l')}_l\right) - \frac{dp}{dx} \tag{10}$$

$$\rho u \frac{\partial T}{\partial x} + \rho v \frac{\partial T}{\partial y} = \frac{\partial}{\partial y}\left(\lambda \frac{\partial T}{\partial y} - \gamma\rho\overline{(v_l'T_l')}_l\right) \tag{11}$$

where

$$-\rho\overline{(u_l'v_l')}_l = \mu_t \frac{\partial u}{\partial y} = \left(\frac{C_\mu f_\mu \rho k_t^2}{\epsilon_t}\right)\frac{\partial u}{\partial y}$$

and

$$-\rho\overline{(v_l'T_l')}_l = \frac{\mu_t}{\text{Pr}_t}\frac{\partial T}{\partial y}$$

The Jones-Launder turbulence model, as derived in the appendix (eqs. (A-26) and (A-27)) for the zone of turbulent spots, in terms of global averages for velocity, is as follows with the assumptions of equation (9):

$$\rho u \frac{\partial k_t}{\partial x} + \rho v \frac{\partial k_t}{\partial y} = \frac{\partial}{\partial y}\left[\left(\mu + \gamma\frac{\mu_t}{\sigma_k}\right)\frac{\partial k_t}{\partial y}\right] + \gamma\mu_t\left(\frac{\partial u}{\partial y}\right)^2$$

$$- \rho\gamma\epsilon_t - 2\mu\left(\frac{\partial k_t^{1/2}}{\partial y}\right)^2 \tag{12}$$

$$\rho u \frac{\partial \epsilon_t}{\partial x} + \rho v \frac{\partial \epsilon_t}{\partial y} = \frac{\partial}{\partial y}\left[\mu + \gamma\frac{\mu_t}{\sigma_k}\frac{\partial \epsilon_t}{\partial y}\right] + C_1 \frac{\epsilon_t}{k_t}\gamma\mu_t\left(\frac{\partial u}{\partial y}\right)^2$$

$$- \rho C_2 f_2 \gamma\frac{\epsilon_t^2}{k_t} + 2\frac{\mu\gamma\mu_t}{\rho}\left(\frac{\partial^2 u}{\partial y^2}\right)^2 \tag{13}$$

Equations (10) to (13) are the simplified equations for the transition region. These equations require the specification of intermittency.

Specification of intermittency requires knowledge of the transition path in terms of the transition start and length. Narasimha (1957) derived from the turbulent spot theory of Emmons (1951) the following transition path equation:

$$\gamma = 1.0 - \exp\left[-4.65\left(\frac{x - x_{tr}}{L_{tr}}\right)^2\right] \quad \text{for } \gamma = 0 \to 0.99 \tag{14}$$

Using the approach of Narasimha (1985) the transition length may be expressed in terms of the transition Reynolds number and a nondimensional spot formation rate as follows:

$$\text{Re}_{L_{tr}} = \frac{2.15}{\sqrt{N}}\text{Re}_{\theta_{tr}}^{3/2} \tag{15}$$

where N, the nondimensional spot formation rate is defined as

$$N = n\sigma\theta_{tr}^3\rho/\mu \tag{16}$$

Narasimha (1985) found that for free-stream turbulence levels greater than 0.1 percent the value of N has the approximate constant value of 0.7×10^{-3}. Equation (15) was used for determining the value of N for free-stream turbulence levels greater than 0.3 percent. For the data of Sohn and Reshotko
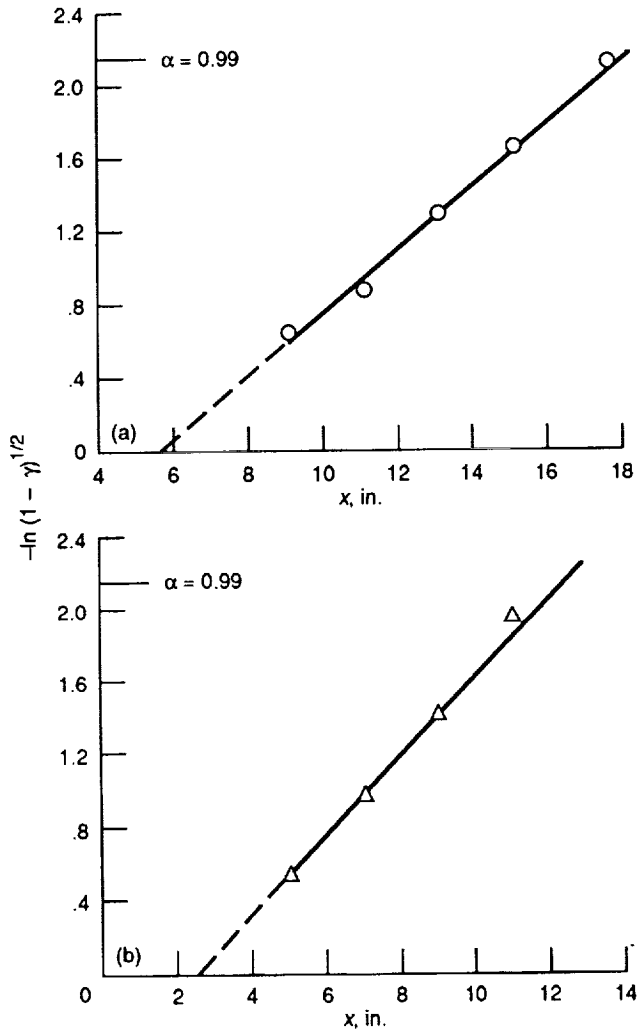
(a) Free-stream turbulence intensity, Tu_e, 1.1 percent; transition length, L_{tr}, 1.03 ft; nondimensional spot formation rate, 0.53×10^{-3}; momentum thickness Reynolds number, $Re_{\theta,tr}$, 337.

(b) Free-stream turbulence intensity, Tu_e, 2.4 percent; transition length, L_{tr}, 0.81 ft; nondimensional spot formation rate, 0.26×10^{-3}; momentum thickness Reynolds number, $Re_{\theta,tr}$, 229.

Figure 2.—Narashimha method for determining $\gamma = 0$ and 0.99 points. (Data from Sohn and Reshotko (1991).)
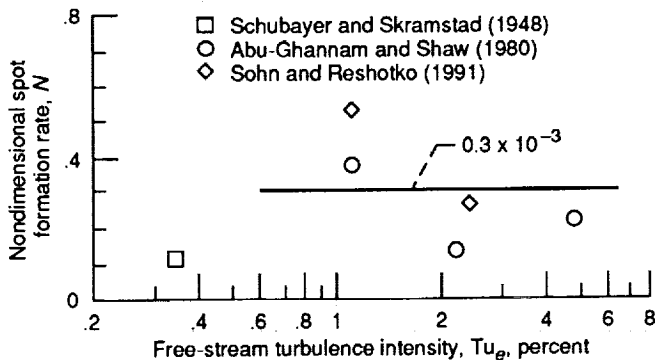

Figure 3.—Variation of nondimensional spot formation rate with free-stream turbulence (Narasimha (1985) method).

(1991), the transition start and length were determined by plotting the intermittency in the manner of Narasimha (1957) and determining the distances x for the 0 and 0.99 intermittency points (fig. 2). The data of Sohn and Reshotko are for cross-stream measurements of turbulence. It is assumed that the turbulence of their experiments was nearly isotropic such that their measured turbulence differs little from the total turbulence as defined in this report. The present work uses a lower value for N of 0.3×10^{-3}, as indicated in figure 3. The use of this value in equation (16) results in the following equation for the calculation of the transition length:

$$Re_{L_{tr}} = 124\ Re_{\theta_{tr}}^{3/2} \qquad \text{for } \gamma = 0 \rightarrow 0.99 \qquad (17)$$

Region 4 (Turbulent Boundary Layer)

Calculations for this region are made using equations (11) and (12) with the intermittency set at one.

Initial and boundary conditions.—Wall boundary condition: Along the wall the no-slip boundary condition was applied as follows:

$$y = 0 \quad : \quad u = v = 0 \qquad (18)$$

For the energy equation a wall heat flux was prescribed.

$$q_w = -K\frac{\partial T}{\partial y}\ (y = 0) \qquad (19)$$

The turbulence kinetic energy and dissipation rate are set to zero at the wall.

$$y = 0 \quad : \quad k = \epsilon = 0 \qquad (20)$$

The zero boundary condition for the dissipation was made possible by Jones and Launder (1970) who added terms to the turbulence energy equation (eqs. (5) and (12)).

Free-stream boundary conditions: The velocity (U_e) and temperature (T_e) were set equal to a constant along the free stream. Boundary conditions for the turbulence kinetic energy and dissipation rate are determined from solving the transport equations (5) and (6) at the edge of the boundary layer.

$$U_e\frac{dk_e}{dx} = -\epsilon_e \qquad (21)$$

$$U_e\frac{d\epsilon}{dx} = C_2\frac{\epsilon_e^2}{k_e} \qquad (22)$$

where initial values of the free-stream turbulence kinetic energy are determined from the turbulence intensity as follows:

$$k_e = 1.5(Tu_eU_e)^2 \qquad (23)$$

where

$$\mathrm{Tu}_e = \frac{\sqrt{1/3(\overline{u'^2} + \overline{v'^2} + \overline{w'^2})}}{U_e}$$

and the initial dissipation rate is determined from

$$\epsilon_e = \frac{k_e^{3/2}}{L_e} \qquad (24)$$

The dissipation length scale L_e can be calculated from the longitudinal integral length scale.

Initial values.—To initiate calculations in region 1, a Blasius velocity profile and a flat temperature profile (unheated start) were used. For the turbulence transport equations, the following initial profiles suggested by Rodi and Scheuerer (1985) were used:

$$k = k_e (u/U_e)^2 \qquad (25)$$

and

$$\epsilon = 0.35k \frac{\partial u}{\partial y} \qquad (26)$$

Results and Discussion

Calculations were performed using the TEXSTAN code for turbulence levels of 1.4, 2.8, and 6.2 percent. The calculations were chosen for comparison with the experimental data of Blair and Werle (1980). They conducted their experiments in a low-speed wind tunnel (100 ft/sec) under ambient air conditions and used grids to generate turbulence. The test section was heated at a rate of 0.078 Btu/ft^2 · sec with an unheated length of 0.141 ft. The experimental boundary conditions used in the calculations are listed in table II. According to Hancock (1980), for grid generated turbulence, the measured values of longitudinal integral length scale can be used to calculate the dissipation length scale as follows:

$$L_e = 1.5\Lambda_e \qquad (27)$$

TABLE II.—BOUNDARY CONDITIONS FOR BLAIR-WERLE DATA

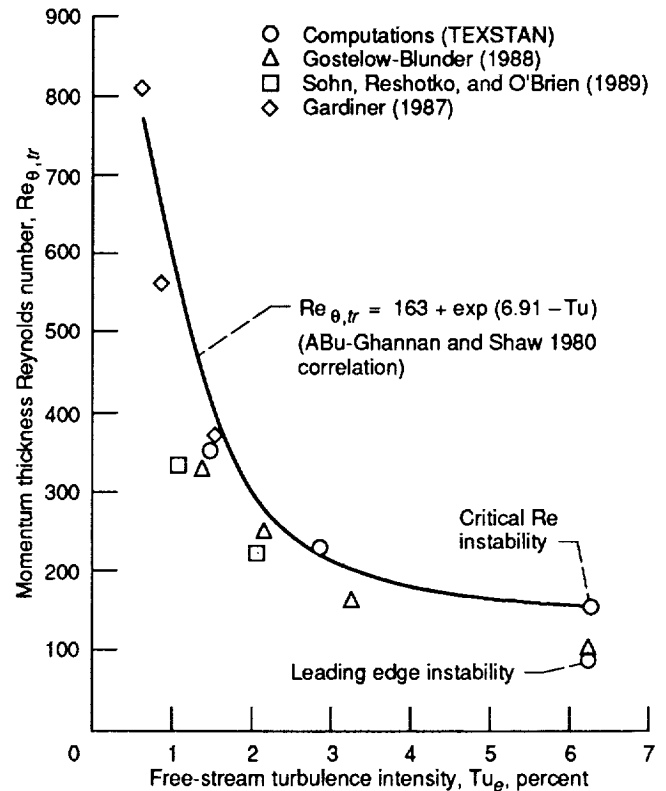| Parameter	Grid 1	Grid 2	Grid 3
Free-stream velocity, U_e, ft/s	100.0	100.0	100.0
Free-stream temperature, T_e, °F	68.5	68.5	68.5
Wall heat flux, q_w, Btu/ft^2/s	0.078	0.078	0.078
Free-stream turbulence intensity, Tu_e, percent	1.4	2.8	6.2
Free-stream turbulence kinetic energy, k_e, ft^2/s^2	2.94	11.8	57.7
Free-stream dissipation rate, ϵ_e, ft^2/s^3	127	511	2450

Figure 4.—Comparison of predicted transition onset with experiments.

Transition Onset

The results of the calculation for the beginning of transition using the equations for region 2 and the criteria for the start of region 2 are given in figure 4. As indicated previously, the initiation of turbulent spots (beginning of region 3) is assumed to occur when the calculations for region 3 show a rapid increase in the skin friction. Also shown in figure 4 are the experimental results of Gardiner (1987), Gostelow and Blunder (1988), Sohn, Reshotko, and O'Brien (1989) and the experimental correlation of Abu-Ghannam and Shaw (1980). Figure 4 shows the effect of assuming stabilizing effects at the leading edge for turbulence levels greater than 5 percent. For the 6.2-percent turbulence level, the present calculations agree with the correlation of Abu-Ghannam and Shaw, if we assume stabilizing influences at the flat-plate leading edge. If we assume that boundary-layer instability begins at the leading edge, and not at the critical Reynolds number for instability, the result is the lower value for transition indicated in figure 4. This is in good agreement with the measured results of Gostelow and Blunder and the observations of Rued and Wittig (1985), Blair and Werle (1980), and Sohn, Reshotko, and O'Brien (1989). As indicated previously, the criterion for the instability beginning at the leading edge for free-stream turbulence levels greater than 5 percent was used in the present calculations. Figure 4 shows general good agreement of experiment and calculations. Gardiner (1987) and Gostelow
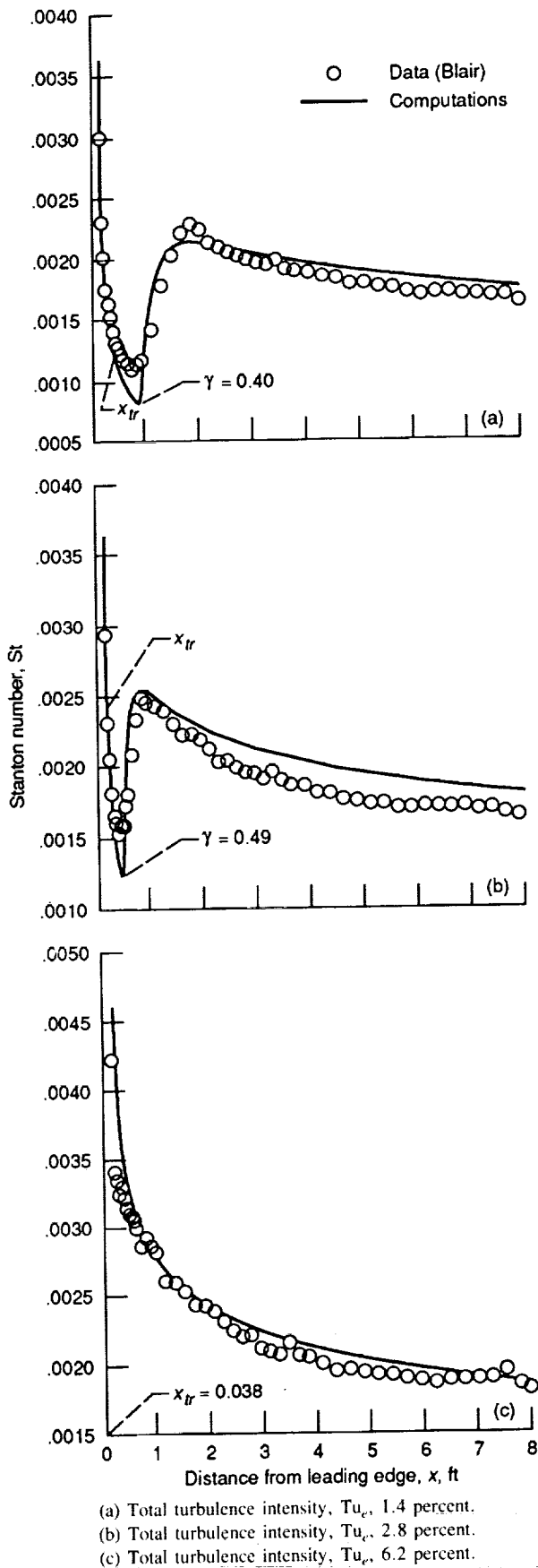
Figure 6.—Skin friction distribution for total turbulence intensity of 6.2 percent.

(a) Total turbulence intensity, Tu_e, 1.4 percent.
(b) Total turbulence intensity, Tu_e, 2.8 percent.
(c) Total turbulence intensity, Tu_e, 6.2 percent.

Figure 5.—Comparison of prediction with experiment (zero pressure gradient).

and Blunder (1988) defined the transition at the 1 percent intermittency level while the transition values of Sohn and Reshotko (1991) are for zero percent intermittency. According to the numerical calculations, this difference in definition should result in a small difference in the Reynolds number (approximately 10 percent), as confirmed by the slightly lower experimental values of Sohn and Reshotko as compared with those of Gostelow and Blunder. As expected, the experimental correlation of Abu-Ghannam and Shaw indicates higher transition values than other experiments, since their definition for transition was based on the onset of deviation from laminar boundary-layer characteristics.

Transition Region

Using the present analysis, as described above, for the beginning of transition permits a determination of when to begin the calculation for region 3. The resulting calculations, using equations (7) to (17), are compared with Blair and Werle's experimental data in figure 5. There is generally good agreement, although the calculated curve swings below the experimental data. This may be the result of neglecting the source terms in the momentum and energy equations (eqs. (7) and (8)) and a result of the presence of high levels of low-frequency unsteadiness in the nonturbulent (laminar) zone of the intermittent boundary layer (Sohn, Reshotko, and O'Brien, 1989), which the models of the present investigation may not have taken into account. Even after spot formation begins, the boundary layer acts as if it were a laminar boundary layer up to intermittency values of 0.40 (1.4 percent case) and 0.49 (2.8 percent case). This finding is consistent with the measured velocity profiles of Sohn, Reshotko, and O'Brien (1989),

which showed a Blasius profile for the laminar zone and a laminar-like profile for the overall profile, for intermittency values up to 0.34 with a 1 percent free-stream turbulence. This finding is also consistent with Gaugler (1985), who had to force transition early in what appeared to be the laminar region in order to agree with the experimental data. With intermittency values greater than 0.34, there is increased deviation from the Blasius velocity profile in the laminar zone. For this reason Sohn, Reshotko, and O'Brien (1989) refer to the laminar zone as a nonturbulent zone to distinguish it from a purely laminar zone.

The increase in heat transfer at substantial values of the intermittency highlights the importance of defining the transition point, since Blair and Werle defined transition as the location where the Stanton number first exceeded the laminar heat-transfer rate. The calculated transition point for the turbulence level of 6.2 percent (fig. 5(b)) occurs before the start of heating; therefore, there is no minimum in the Stanton number. This minimum becomes apparent if the calculated skin friction in the unheated length is plotted (fig. 6).

Concluding Remarks

The present work has examined the ability of two-equation turbulence models to simulate the onset of bypass transition and the region of transition consisting of islands of turbulent spots in a sea of laminar-like fluid. A critical test for a turbulence model is its ability to simulate disturbance growth, which is governed by the free-stream turbulence energy, and to determine the onset of transition. The Jones-Launder turbulence model has performed this job well and suggests that models for bypass transition need to comprehend the relationship between disturbance growth and the convection, diffusion, and production of turbulence in the boundary layer. The intermittent flow of the transition region was modeled by the use of conditioned flow equations rather than by global time-averaged equations. These equations better express the physics of turbulent spot-fluid interaction and produce a more complete and accurate description of turbulent energy budgets. In addition, they bring out the necessary and strong role that intermittency plays in calculating heat transfer with transition without the need to modify the turbulence production term as others have done (Schmidt and Patankar (1988)).

It appears that the existence and length of the laminar boundary layer at the leading edge of a flat plate depends on the presence of stabilizing or destabilizing effects. This suggests that application of the present work to turbine blades will require additional information on and modeling of the effect of curvature and pressure gradient on the stability of the laminar boundary layer. In the present effort for flow over a flat plate, it is assumed that nonlinear growth for free-stream turbulence levels less than 5 percent begins at the critical Reynolds number for linear stability. It is not clear that one is justified in this assumption. It is quite possible, as previously suggested, that the condition for the beginning of nonlinear growth is dependent on the free-stream turbulence level in addition to the effects of curvature and pressure gradient. There is a need in this area for more experimental and analytical information.

Lewis Research Center
National Aeronautics and Space Administration
Cleveland, Ohio, April 28, 1991

Appendix—Transition Region Equations

The development of equations for the transition region uses the approach of Vancoillie and Dick (1988), who developed conditioned continuity, momentum, and turbulence equations for the intermittent flow in the transition region. In this appendix the conditioned equations for the energy equation are derived and the conditioned equations are combined to permit the calculation of global values.

Vancoillie and Dick used an intermittency function $I(x,y,z,t)$ for their conditioning analysis, with the function having a value of 1 inside the turbulent spot and 0 outside. The time average of I is the intermittency factor. Conditioned averages are defined by

$$\overline{u_t} = \frac{\overline{uI}}{\gamma} \qquad \overline{u_l} = \frac{\overline{u(1-I)}}{1-\gamma} \tag{A-1}$$

where

$$\gamma = \frac{1}{t} \int_0^t I\,dt = \overline{I} \tag{A-2}$$

By using equation (A-1), the following global averages may be developed:

$$\overline{u} = \gamma\overline{u_t} + (1-\gamma)\overline{u_l} \tag{A-3}$$

and

$$\overline{v} = \gamma\overline{v_t} + (1-\gamma)\overline{v_l} \tag{A-4}$$

In what follows, the use of a bar for simple symbols is omitted for convenience.

Continuity Equations

Vancoillie and Dick's derivation of the continuity equations is

$$\frac{\partial \gamma u_t}{\partial x} + \frac{\partial \gamma v_t}{\partial y} = \frac{\overline{dI}}{dt} \tag{A-5}$$

and

$$\frac{\partial(1-\gamma)u_l}{\partial x} + \frac{\partial(1-\gamma)v_l}{\partial y} = -\frac{\overline{dI}}{dt} \qquad \text{(A-6)}$$

Equations (A-5) and (A-6) may be combined, and using equation (A-2) and (A-3) results in the following global average continuity equation:

$$\frac{\partial u}{\partial x} + \frac{\partial v}{\partial y} = 0 \qquad \text{(A-7)}$$

Momentum Equations

The modeled momentum equations of Vancoillie and Dick are

$$\rho\gamma u_t \frac{\partial u_t}{\partial x} + \rho\gamma v_t \frac{\partial u_t}{\partial y} = -\gamma \frac{\partial p}{\partial x} + \gamma \frac{\partial}{\partial y}\left[\mu \frac{\partial u_t}{\partial y} - \rho\overline{(u_t'v_t')}_t\right]$$

$$+ \rho(u_l - u_t)u_l \frac{d\gamma}{dx} + c_v\mu \frac{u_l - u_t}{\delta^*}\frac{d\gamma}{dx} \qquad \text{(A-8)}$$

and

$$\rho(1-\gamma)u_l \frac{\partial u_l}{\partial x} + \rho v_l(1-\gamma) \frac{\partial u_l}{\partial y} = -(1-\gamma) \frac{\partial p}{\partial x}$$

$$+ (1-\gamma) \frac{\partial}{\partial y}\left[\mu \frac{\partial u_l}{\partial y} - \rho\overline{(u_l'v_l')}_l\right] - c_v\mu \frac{u_l - u_t}{\delta^*}\frac{d\gamma}{dx}$$

$$\text{(A-9)}$$

Vancoillie and Dick solved equations (A-8) and (A-9) (neglecting the Reynolds stresses of laminar zone) to predict for the transition region, boundary-layer thickness factors, velocity, and turbulence intensity profiles. Since it is the objective of the present work to determine the combined effect of turbulent spots and the laminar zone on heat transfer in the transition region, the individual equations for each zone are combined to obtain global values.

Combining equations (A-8) and (A-9) and using equations (A-3) and (A-4) and the following derivatives of equations (A-3) and (A-4)

$$\frac{\partial u}{\partial x} = \gamma \frac{\partial u_t}{\partial x} + (1-\gamma) \frac{\partial u_l}{\partial x} + (u_t - u_l) \frac{d\gamma}{dx} \qquad \text{(A-10)}$$

$$\frac{\partial u}{\partial y} = \gamma \frac{\partial u_t}{\partial y} + (1-\gamma) \frac{\partial u_l}{\partial y} \qquad \text{(A-11)}$$

result in the equation of global-averaged and conditioned-averaged variables:

$$\rho u \frac{\partial u}{\partial x} + \rho v \frac{\partial u}{\partial y} = -\frac{dp}{dx} + \frac{\partial}{\partial y}\left[\mu \frac{\partial u}{\partial y} - \gamma\rho\overline{(u_t'v_t')}_t\right.$$

$$\left. - (1-\gamma)\rho\overline{(u_l'v_l')}_l\right] + \rho\gamma\left[(u_l - u_t)\left(\frac{\partial u_t}{\partial x} - \frac{\partial u}{\partial x}\right)\right.$$

$$\left. + (v_l - v_t)\left(\frac{\partial u_t}{\partial y} - \frac{\partial u}{\partial y}\right)\right] \qquad \text{(A-12)}$$

Energy equations

The procedure for determining the time averaged conditioned energy equations follows that used by Vancoillie and Dick for the conditioned momentum equations. The Navier-Stokes energy equation is multiplied by I (turbulent zone) and $1 - I$ (laminar zone), and the total derivative for I is multiplied by T_t' and T_l' for the turbulent and laminar zone, respectively. The equations are added and time averaged. Some terms are neglected on the basis of boundary-layer approximations and two-dimensional flow. The result is as follows:

$$\rho\gamma u_t \frac{\partial T_t}{\partial x} + \rho\gamma v_t \frac{\partial T_t}{\partial y} = \gamma \frac{\partial}{\partial y}\left[\lambda \frac{\partial T_t}{\partial y} - \rho\overline{(v_t'T_t')}_t\right]$$

$$- \lambda\overline{\frac{\partial T_t'}{\partial x}\frac{\partial I}{\partial x}} - \lambda\overline{\frac{\partial T_t'}{\partial z}\frac{\partial I}{\partial z}} + \overline{\rho T_t'\frac{dI}{dt}} \qquad \text{(A-13)}$$

for the turbulent zone and

$$\rho(1-\gamma)u_l \frac{\partial T_l}{\partial x} + \rho(1-\gamma)v_l \frac{\partial T_l}{\partial y} = (1-\gamma) \frac{\partial}{\partial y}\left[\lambda \frac{\partial T_l}{\partial y}\right.$$

$$\left. - \rho\overline{(v_l'T_l')}_l\right] + \lambda\overline{\frac{\partial T_l'}{\partial x}\frac{\partial I}{\partial x}} + \lambda\overline{\frac{\partial T_l'}{\partial z}\frac{\partial I}{\partial z}} - \overline{\rho T_l'\frac{dI}{dt}}$$

$$\text{(A-14)}$$

for the laminar zone.

The first two source terms in equations (A-13) and (A-14) may be modeled in the manner of Vancoillie and Dick, resulting in

$$\rho\gamma u_t \frac{\partial T_t}{\partial x} + \rho\gamma v_t \frac{\partial T_t}{\partial y} = \gamma \frac{\partial}{\partial y}\left[\lambda \frac{\partial T_t}{\partial y} - \rho\overline{(v_t'T_t')}_t\right]$$

$$\frac{c_T\lambda}{\delta_3}(T_l - T_t) \frac{d\gamma}{dx} + \overline{\rho T_t'\frac{dI}{dt}} \qquad \text{(A-15)}$$

and

$$\rho(1 - \gamma)u_l \frac{\partial T_l}{\partial x} + \rho(1 - \gamma)v_l \frac{\partial T_l}{\partial y}$$

$$= (1 - \gamma) \frac{\partial}{\partial y} \left[\lambda \frac{\partial T_l}{\partial y} - \rho \overline{(v_l' T_l')}_l \right]$$

$$- \frac{c_T \lambda}{\delta_3} (T_l - T_t) \frac{d\gamma}{dx} + \overline{\rho T_l' \frac{dI}{dt}} \qquad (A-16)$$

Combining equations (A-15) and (A-16) results in

$$\rho\gamma u_t \frac{\partial T_t}{\partial x} + \rho(1 - \gamma)u_l \frac{\partial T_l}{\partial x} + \rho\gamma v_t \frac{\partial T_t}{\partial y} + \rho(1 - \gamma)v_l \frac{\partial T_l}{\partial y}$$

$$= \gamma \frac{\partial}{\partial y} \left[\lambda \frac{\partial T_t}{\partial y} - \rho \overline{(v_t' T_t')}_t \right] + (1 - \gamma) \frac{\partial}{\partial y} \left[\lambda \frac{\partial T_l}{\partial y} \right.$$

$$\left. - \rho \overline{(v_l' T_l')}_l \right] + \overline{\rho T_t' \frac{dI}{dt}} - \overline{\rho T_l' \frac{dI}{dt}} \qquad (A-17)$$

The source terms at the end of equation (A-17) result from the interaction between the turbulent and laminar zones. These terms are modeled according to the method of Vancoillie and Dick. They assumed that the intermittency function at the interface between the laminar zone and turbulent spot changed linearly from 0 to 1 over a finite interval that goes mathematically to zero and that the flow velocity at the interface is equal to the laminar zone averaged velocity u_l. With these assumptions the above source terms may be expressed as follows:

$$\overline{\rho T_t' \frac{dI}{dt}} - \overline{\rho T_l' \frac{dI}{dt}} = (T_l - T_t)u_l \frac{d\gamma}{dx} \qquad (A-18)$$

Treating equation (A-17) in the same manner as the momentum equations (A-8) and (A-9) and using the following equations

$$T = \gamma T_t + (1 - \gamma)T_l \qquad (A-19)$$

$$\frac{\partial T}{\partial x} = \gamma \frac{\partial T_t}{\partial x} + (1 - \gamma) \frac{\partial T_l}{\partial x} + (T_t - T_l) \frac{d\gamma}{dx} \qquad (A-20)$$

$$\frac{\partial T}{\partial y} = \gamma \frac{\partial T_t}{\partial y} + (1 - \gamma) \frac{\partial T_l}{\partial y} \qquad (A-21)$$

$$\frac{\partial^2 T}{\partial y^2} = \gamma \frac{\partial^2 T_t}{\partial y^2} + (1 - \gamma) \frac{\partial^2 T_l}{\partial y^2} \qquad (A-22)$$

result in an energy equation expressed in terms of global and conditional averages as follows:

$$\rho u \frac{\partial T}{\partial x} + \rho v \frac{\partial T}{\partial y} = \frac{\partial}{\partial y} \left[\lambda \frac{\partial T}{\partial y} - \rho\gamma \overline{(v_t' T_t')}_t \right.$$

$$\left. - \rho(1 - \gamma)\overline{(v_l' T_l')}_l \right] + \rho\gamma(u_l - u_t) \left[\frac{\partial T_t}{\partial x} - \frac{\partial T}{\partial x} \right]$$

$$+ \rho\gamma(v_l - v_t) \left[\frac{\partial T_t}{\partial y} - \frac{\partial T}{\partial y} \right] \qquad (A-23)$$

Jones-Launder Turbulence Model

The Jones-Launder turbulence kinetic energy model derived by Vancoillie and Dick for the turbulent zone is

$$\rho\gamma u_t \frac{\partial k_t}{\partial x} + \rho\gamma v_t \frac{\partial k_t}{\partial y} = \gamma \frac{\partial}{\partial y} \left[\left(\mu + \frac{\mu_t}{\sigma_k} \right) \frac{\partial k_t}{\partial y} \right]$$

$$+ \gamma\mu_t \left(\frac{\partial u_t}{\partial y} \right)^2 - \rho\gamma\epsilon_t - \gamma 2\mu \left(\frac{\partial k_t^{1/2}}{\partial y} \right)^2$$

$$+ c_k \mu_t \frac{(u_l - u_t)^2}{\delta^*} \frac{d\gamma}{dx} \qquad (A-24)$$

It follows that the equation for the laminar zone is

$$\rho(1 - \gamma)u_l \frac{\partial k_l}{\partial x} + \rho(1 - \gamma)v_l \frac{\partial k_l}{\partial y} = (1 - \gamma) \frac{\partial}{\partial y} \left[\mu \frac{\partial k_l}{\partial y} \right]$$

$$+ (1 - \gamma)\mu_l \left(\frac{\partial u_l}{\partial y} \right)^2 - \rho(1 - \gamma)\epsilon_l$$

$$- (1 - \gamma)2\mu \left(\frac{\partial k_l^{1/2}}{\partial y} \right)^2 - c_k \mu_l \frac{(u_l - u_t)^2}{\delta^*} \frac{d\gamma}{dx}$$

$$(A-25)$$

Equations (A-24) and (A-25) are combined and simplified as previously. To permit simplification, we assume

$$\frac{\partial k_t}{\partial x} = \frac{\partial k_l}{\partial y}$$

$$\frac{\partial k_t}{\partial y} = \frac{\partial k_l}{\partial y}$$

This suggests that the disturbance energies in the laminar zone are related linearly to those occurring in the turbulent spots. Experimental data (Sohn, Reshatko, and O'Brien, 1989, and others) seem to confirm this. The turbulence dissipation and turbulence viscosity terms for the laminar zone are small compared with the same terms for the turbulent zone and are therefore neglected. The result of combining is

$$\rho u \frac{\partial k_l}{\partial x} + \rho v \frac{\partial k_l}{\partial y} = \frac{\partial}{\partial y} \left[\left(\mu + \gamma \frac{\mu_t}{\sigma_k} \right) \frac{\partial k_l}{\partial y} \right] + \gamma \mu_t \left(\frac{\partial u_l}{\partial y} \right)^2$$
$$- \rho \gamma \epsilon_l - 2\mu \left(\frac{\partial k_l^{1/2}}{\partial y} \right)^2 \qquad \text{(A-26)}$$

Approaching the turbulence dissipation equations in the same manner as for the turbulence kinetic energy we have

$$\rho u \frac{\partial \epsilon_l}{\partial x} + \rho v \frac{\partial \epsilon_l}{\partial y} = \frac{\partial}{\partial y} \left[\left(\mu + \gamma \frac{\mu_t}{\sigma_k} \right) \frac{\partial \epsilon_l}{\partial y} \right]$$
$$+ C_1 \frac{\epsilon_l}{k_l} \gamma \mu_t \left(\frac{\partial u_l}{\partial y} \right)^2 - \rho C_2 f_2 \gamma \frac{\epsilon_l^2}{k_l} + 2 \frac{\mu \gamma \mu_t}{\rho} \left(\frac{\partial^2 u_l}{\partial y^2} \right)$$

$$\text{(A-27)}$$

References

Abu-Ghannam, B.J.; and Shaw, R. (1980): Natural Transition of Boundary Layers—The Effects of Turbulence, Pressure Gradient, and Flow History. J. Mech. Eng. Science, vol. 22, no. 5.

Blair, M.F.; and Werle, M.J. (1980): The Influence of Free-Stream Turbulence on the Zero Pressure Gradient Fully Turbulent Boundary Layer. UTRC report R80-914388-12.

Cebeci, T.; and Smith, A.M.O. (1974): Analysis of Turbulent Boundary Layers, Academic Press.

Chen, K.K.; and Thyson, N.A. (1971): Extension of Emmon's Spot Theory to Flows on Blunt Bodies. AIAA J., vol. 9, no. 5.

Crawford, M.E.; and Kays, W.M. (1976): STAN5—A Program for Numerical Computation of Two-dimensional Internal and External Boundary Layer Flows. NASA CR-2742.

Crawford, M.E. (1985): TEXSTAN program, Univ. of Texas at Austin.

Dey, J.; and Narasimha, R. (1984): Transition Zone Length in Incompressible Boundary Layers. Indian Institute of Science, Bangalore, India, Report 84-FM-91.

Dey, J.; and Narasimha, R. (1988): An Integral Method for the Calculation of 2-D Transitional Boundary Layers. Indian Institute of Science, Bangalore, India, Report 88-FM-7.

Dhawan, S.; and Narasimha, R. (1958): Some Properties of Boundary Layer Flow During the Transition from Laminar to Turbulent Motion. J. Fluid Mech., vol. 3, pt. 4, pp. 418-436.

Donaldson, C.D. (1969): A Computer Study of an Analytical Model of Boundary Layer Transition. AIAA J., vol. 7, no. 2.

Dyban, E.P.; Epik, E. YA.; and Suprun, T.T. (1976): Characteristics of the Laminar Boundary Layer in the Presence of Elevated Free-Stream Turbulence. Fluid Mech.-Sov. Res., vol. 5, no.4.

Elder, J.W. (1960): An Experimental Investigation of Turbulent Spots and Breakdown to Turbulence. J. Fluid Mech., vol.9, pp. 235-246.

Emmons, H.W. (1951): The Laminar-Turbulent Transition in a Boundary Layer. Part I. J. Aeronaut. Sci., vol. 18, no. 7, pp. 490-498.

Gardiner, I.D. (1987): Transition in Boundary Layer Flows. Ph.D. thesis, Dundee College of Technology.

Gaugler, R.E. (1985): A Review and Analysis of Boundary Layer Transition Data for Turbine Applications. ASME paper 85-GT-83 (also NASA TM-86880).

Gostelow, J.P.; and Blunder, A.R. (1988): Investigations of Boundary-Layer Transition in an Adverse Pressure Gradient. Turbine and Aeroengine Congress. The Netherlands.

Hancock, P.E. (1980): Effect of Free-Stream Turbulence on Turbulent Boundary Layers. Ph.D. Thesis, Imperial College, London Univ.

Jones, W.P.; and Launder, B.E. (1973): The Calculation of Low-Reynolds Number Phenomena With a Two-Equation (Model) of Turbulence. Int. J. Heat Mass Transfer, vol.16, pp. 1119-1130.

Kim, J.; Simon, T.; Kestoras, M. (1989): Fluid Mechanics and Heat Transfer Measurements in Transitional Boundary Layers Conditionally Sampled on Intermittency. Proceedings of the National Heat Transfer Conference.

McDonald, H.; and Fish. R.W. (1973): Practical Calculations of Transitional Boundary Layers. Int. J. Heat Mass Trans., vol.16, pp. 1729-1744.

Morkovin, M.V. (1978): Instability Transition to Turbulence and Predictability. AGARD AG-236 (avail. NTIS, AD-A057834).

Narasimha, R. (1957): On the Distribution of Intermittency in the Transition Region of a Boundary Layer. J. Aeronaut. Sci., vol. 24, no. 9, pp. 711-712.

Narasimha, R. (1985): The Laminar-Turbulent Transition Zone in the Boundary Layer. Progress in Aerospace Science, vol. 22, pp. 29-80.

Patankar, S.V.; and Spalding, D.B. (1970): Heat and Mass Transfer in Boundary Layers—A General Calculation Procedure. 2nd ed., Interext Books, London.

Reshotko, E. (1986): Stability and Transition, How Much Do We Know? Tenth U.S. National Congress of Applied Mechanics, J.P. Lamb, ed., ASME, pp. 421-434.

Rodi, W.; and Scheurer, G. (1985): Calculation of Laminar-Turbulent Boundary Layer Transition on Turbine Blades. Proc. Heat Transfer and Cooling in Gas Turbines, AGARD CP-390, AGARD, Nevilly-Sur-Seine, France, pp. 18-1—18-13.

Rued, K.; and Wittig, S. (1985): Free Stream Turbulence and Pressure Gradient Effects on Heat Transfer and Boundary Layer Development on Highly Cooled Surfaces. J. Eng. Gas Turbines Power, vol. 107, no.1, pp. 54-59.

Schbauer, G.B.; and Skramstad, H.K. (1948): Laminar-Boundary Layer Oscillations and Transition on a Flat Plate. NACA Report 909.

Schmidt, R.C.; and Patankar, S.V. (1988): Two-Equation Low-Reynolds-Number Turbulence Modeling of Transitional Boundary Layer Flows Characteristic of Gas Turbine Blades. NASA CR-4145.

Sohn, K-H (1986): Transition in a Disturbed Environment. M.S. thesis, Case Western Reserve University.

Sohn, K-H.; Reshotko, E.; and O'Brien, J.E. (1989): Some Characteristics of Bypass Transition in a Heated Boundary Layer. Seventh Symposium on Turbulent Shear Flows, Vol. 1, Pennsylvania State University, pp. 2.4.1-2.4.6.

Sohn, K-H; and Reshotko, E. (1991): Experimental Study Of Boundary Layer Transition With Elevated Freestream Turbulence On A Heated Flat Plate. NASA CR-187068.

Vancoillie, G.; and Dick, E. (1988): A Turbulence Model for the Numerical Simulation of the Transition Zone in a Boundary Layer. Int. J. Eng. Fluid Mech., vol. 1, no. 1.

REPORT DOCUMENTATION PAGE

1. AGENCY USE ONLY (Leave blank)	2. REPORT DATE	3. REPORT TYPE AND DATES COVERED
	October 1991	Technical Paper

4. TITLE AND SUBTITLE

Modeling of the Heat Transfer in Bypass Transitional Boundary-Layer Flows

5. FUNDING NUMBERS

WU - 505 - 62 - 52

6. AUTHOR(S)

Frederick F. Simon and Craig A. Stephens

7. PERFORMING ORGANIZATION NAME(S) AND ADDRESS(ES)

National Aeronautics and Space Administration
Lewis Research Center
Cleveland, Ohio 44135 - 3191

8. PERFORMING ORGANIZATION REPORT NUMBER

E - 6046

9. SPONSORING/MONITORING AGENCY NAMES(S) AND ADDRESS(ES)

National Aeronautics and Space Administration
Washington, D.C. 20546 - 0001

10. SPONSORING/MONITORING AGENCY REPORT NUMBER

NASA TP - 3170

11. SUPPLEMENTARY NOTES

Frederick F. Simon, Lewis Research Center. Craig A. Stephens is presently with PRC, Inc., P.O. Box 273, Edwards, California 93523. Responsible person, Frederick F. Simon, (216) 433 - 5894.

12a. DISTRIBUTION/AVAILABILITY STATEMENT

Unclassified - Unlimited
Subject Category 34

12b. DISTRIBUTION CODE

13. ABSTRACT (Maximum 200 words)

A low Reynolds number k-ϵ turbulence model and conditioned momentum, energy and turbulence equations were used to predict bypass transition heat transfer on a flat plate in a high-disturbance environment with zero pressure gradient. The use of conditioned equations has been demonstrated by other researchers to be an improvement over the use of the global-time-averaged equations for the calculation of velocity profiles and turbulence intensity profiles in the transition region of a boundary layer. The present work extends the approach of conditioned equations to include heat transfer and uses a modeling of transition events to predict transition onset and the extent of transition on a flat plate. The events, which describe the boundary layer at the leading edge, result in boundary-layer regions consisting of (1) the laminar, (2) pseudolaminar, (3) transitional, and (4) turbulent boundary layers. The modeled transition events were incorporated into the TEXSTAN two-dimensional boundary-layer code which is used to numerically predict the heat transfer. The numerical predictions in general compared well with the experimental data and revealed areas where additional experimental information is needed.

14. SUBJECT TERMS			15. NUMBER OF PAGES
Heat transfer; Transition; Boundary layer			16
			16. PRICE CODE A03

17. SECURITY CLASSIFICATION OF REPORT	18. SECURITY CLASSIFICATION OF THIS PAGE	19. SECURITY CLASSIFICATION OF ABSTRACT	20. LIMITATION OF ABSTRACT
Unclassified	Unclassified	Unclassified	